with four short equivalent Co–Co bonds and two longer equivalent Co–Co bonds. Hence, the nonconformity of the Co_4N_4 core to a tetragonal D_{2d} geometry with four equivalent short Co–Co distances is *not* consistent with the predicted first-order Jahn–Teller effect.[5]

The close resemblance of the structural parameters of $Co_4(NO)_4(\mu_3\text{-}NC(CH_3)_3)_4$ to an orthorhombic D_2 geometry is indicative that effects more systematic than those of anisotropic crystal-packing forces or internal intramolecular steric pressures are operative in this case to produce the observed deviations from the predicted D_{2d} geometry.[6,7] The weak second-order Jahn–Teller effect[8] can produce perturbations on molecular geometry by vibronic coupling of the ground state and low-lying excited states of the same spin multiplicity. Both Pearson[9] and Mingos[10] have utilized the second-order Jahn–Teller effect to rationalize the structures of molecules. The vibrations which can produce such a second-order distortion must be contained in the direct product of the symmetry species of the ground and excited states. On the basis of the reasonable assumption that a first-order Jahn–Teller mechanism has provided a tetragonal D_{2d} geometry such that the HOMO containing the four antibonding metal clusters electrons is a doubly degenerate e orbital and with higher unoccupied b_2, e, and a_2 *antibonding* MO's, only the direct product e $\times$ e contains the B_1 mode which is the normal mode of vibration consistent with a deformation from D_{2d} to D_2 geometry.

The plausibility of these qualitative arguments is contingent upon a quantitative approach to the bonding in $Co_4(NO)_4(\mu_3\text{-}NC(CH_3)_3)_4$.[11,12] Whether the D_2 geometry, instead of the D_{2d} one expected for a system of this particular MO-electronic configuration, is unique to this molecule or is also characteristic of other electronically equivalent cubane-like systems must await fur-

ther structural studies. In this connection a vigorous effort is being made to prepare the unknown $Co_4(NO)_4$-$(\mu_3\text{-}S)_4$ analog. The work presented here will be reported in full upon completion of closely related research which will include the characterization of the recently prepared monocation of $Co_4(NO)_4(\mu_3\text{-}NC(CH_3)_3)_4$ as well as the preparation and structural analysis of the cubane-like $Co_4(NO)_4(\mu_3\text{-}NR)_3(\mu_3\text{-}SNR)$ molecule (where R = $C(CH_3)_3$), a unique complex involving the replacement of one NR ligand with a SNR ligand which is also electronically equivalent to a triply bridging disulfide ligand.

Robert S. Gall, Neil G. Connelly, Lawrence F. Dahl*
Department of Chemistry, University of Wisconsin
Madison, Wisconsin 53706
Received February 14, 1974

Preparation, Structure, and Bonding of Two Cubane-Like Iron–Nitrosyl Complexes, $Fe_4(NO)_4(\mu_3\text{-}S)_4$ and $Fe_4(NO)_4(\mu_3\text{-}S)_2(\mu_3\text{-}NC(CH_3)_3)_2$. Stereochemical Consequences of Bridging Ligand Substitution on a Completely Bonding Tetrametal Cluster Unit and of Different Terminal Ligands on the Cubane-Like Fe_4S_4 Core

Sir:

We wish to report the preparation and structures of two closely related cubane-like iron nitrosyl clusters, $Fe_4(NO)_4(\mu_3\text{-}S)_4$ and $Fe_4(NO)_4(\mu_3\text{-}S)_2(\mu_3\text{-}NC(CH_3)_3)_2$. The latter differs from the former by the presence of two triply bridging *N-tert*-butyl groups instead of two electronically equivalent, triply bridging sulfur atoms. This work was a direct consequence of our desire to assess (and thereby hopefully to differentiate) between a possible second-order Jahn-Teller effect and unusual steric effects of the *N-tert*-butyl ligands on the recently determined geometry of the cubane-like $Co_4(NO)_4(\mu_3\text{-}NC(CH_3)_3)_4$ molecule[1] by the synthesis and structural

(5) R. W. Jotham and S. F. A. Kettle, *Inorg. Chim. Acta*, **5**, 183 (1971). A distortion from a cubic T_d to a tetragonal D_{2d} geometry *via* an E mode vibration is possible as the E representation in T_d correlates with the totally symmetric A_1 representation under tetragonal D_{2d} symmetry. However, a distortion from a cubic T_d to an orthorhombic D_2 geometry is not allowed by the first-order Jahn–Teller effect, even though the E representation of T_d symmetry correlates with the (A + A) representation under D_2 symmetry, due to the tetragonal D_{2d} point group being an intermediate point group.

(6) Considerable variations of 0.1 Å in metal–metal distances have been observed in the solid state for cubane-like tetramers containing a nonbonding tetrahedron of metal atoms (e.g., $Co_4(\eta\text{-}C_5H_5)_4(\mu_3\text{-}S)_4$,[1a] $Os_4(CO)_{12}(\mu_3\text{-}O)_4$,[7a] and $Re_4(CO)_{12}(\mu_3\text{-}SCH_3)_4$[7b]). Although the observed differences in the nonbonding metal–metal distances in each of these molecules are statistically significant, there is no *chemical* significance in the observed nonsystematic variations from an idealized cubic T_d geometry aside from the presumed anisotropic steric effects. It has been pointed out[1a] that maximum variations are expected and found for metal–metal distances for which the *net* metal–metal interactions are nonbonding. In the case of $Co_4(NO)_4(\mu_2\text{-}NC(CH_3)_3)_4$ it is presumed from potential energy considerations that the metal–metal bonding (manifested by the short Co–Co distances) would lead to a relatively rigid Co_4N_4 core for which it then is difficult to reconcile the observed D_2 deformation from a tetragonal D_{2d} geometry as arising from only interligand repulsions (with complete neglect of electronic effects).

(7) (a) D. Bright, *Chem. Commun.*, 1169 (1970); (b) E. W. Abel, W. Harrison, R. A. N. McLean, C. Marsh, and J. Trotter, *ibid.*, 1531 (1970); W. Harrison, W. C. Marsh, and J. Trotter, *J. Chem. Soc., Dalton Trans.*, 1009 (1972).

(8) (a) U. Öpik and M. H. L. Pryce, *Proc. Roy. Soc., Ser. A*, **238**, 425 (1957); (b) R. F. W. Bader, *Can. J. Chem.*, 40, 1164 (1962).

(9) R. G. Pearson, *J. Amer. Chem. Soc.*, **91**, 4947 (1969).

(10) D. M. P. Mingos, *Nature (London), Phys. Sci.*, **229**, 193 (1971).

(11) Molecular orbital calculations of these metal cluster systems (including the terminal ligands) are being performed *via* the nonparameterized Fenske–Hall model[12] in order to determine the degree of validity of our currently utilized qualitative metal cluster model (which allows complete electron delocalization only among the metal atoms).

(12) M. B. Hall and R. F. Fenske, *Inorg. Chem.*, **11**, 768 (1972).

(1) R. S. Gall, N. G. Connelly, and L. F. Dahl, *J. Amer. Chem. Soc.*, **96**, 4017 (1974).

Table I. Selected Mean Distances and Bond Angles for Several Cubane-Like Iron Tetramers[a,b]

	Fe4(NO)4(μ3-S)4[c]	Fe4(NO)4(μ3-S)2(μ3-NR)2[c] R = C(CH3)3	Fe4(η-C5H5)4(μ3-S)4[d] (monoclinic form)	[Fe4(SR)4(μ3-S)4]2-[e] R = CH2C6H5
Fe4B4 core	Fe4S4	Fe4S2N2	Fe4S4	Fe4S4
Crystallographic site symmetry	Ci-1	Cs-m	C2-2	Ci-1
Idealized geometry of Fe4B4 core	Td-43m	C2v-2mm	D2d-42m	D2d-42m
Fe–Fe	[6] 2.634 (1) (B = S)	[1] 2.642 (1) (B = B' = S) [4] 2.562 (1) (B = S; B' = N) [1] 2.496 (1) (B = B' = N)	[2] 2.650 (6) (B = S) [4] 3.363 (10)	[2] 2.776 (2) (B = S) [4] 2.731 (1)
B···B'	[6] 3.503 (2) (B = S)	[1] 3.507 (3) (B = B' = S) [4] 3.208 (4) (B = S; B' = N) [1] 2.880 (7) (B = B' = N)	[4] 2.880 (12) (B = S) [2] 3.334 (9)	[2] 3.645 (3) (B = S) [4] 3.586 (2)
Fe–B	[12] 2.217 (2) (B = S)	[4] 2.224 (2) (B = S) [2] 2.222 (2) (B = S) [2] 1.914 (3) (B = N) [4] 1.908 (3) (B = N)	[8] 2.204 (8) (B = S) [4] 2.250 (10)	[8] 2.310 (2) (B = S) [4] 2.239 (2)
Fe–B–Fe	[12] 73.4 (1) (B = S)	[2] 72.9 (1) (B = S) [4] 70.4 (1) (B = S) [4] 84.2 (1) (B = N) [2] 81.6 (1) (B = N)	[4] 73.9 (2) (B = S) [8] 98.0 (3)	[4] 73.9 (1) (B = S) [8] 73.8 (1)
B–Fe–B'	[12] 104.4 (1) (B = S)	[2] 104.0 (1) (B = B' = S) [4] 101.4 (1) (B = S; B' = N) [4] 101.6 (1) (B = N; B' = S) [2] 98.0 (2) (B = B' = N)	[8] 80.6 (3) (B = S) [4] 98.2 (2)	[4] 104.2 (1) (B = S) [8] 104.0 (1)

[a] Each esd given in parentheses represents that of a single observation rather than an estimated standard deviation of the mean. [b] Brackets [ ] means the number of bond distances or angles having the values listed in the right column. [c] This work. [d] Reference 7. [e] Reference 2.
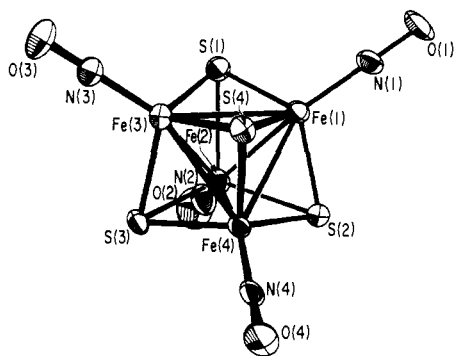

Figure 1. The cubane-like Fe4(NO)4(μ3-S)4 molecule which experimentally possesses cubic T_d symmetry with the Fe4S4 core containing a completely bonding iron tetrahedron.

examination of the completely bonding tetrairon analogs, Fe4(NO)4(μ3-X)4 (where X = NC(CH3)3 and S), in that from only electronic considerations both should have a cubic T_d Fe4B4 central core (where B = N or S). Unfortunately, this initial goal has not yet been reached in that to date we have succeeded in preparing and isolating Fe4(NO)4(μ3-S)4 but not Fe4(NO)4(μ3-NC(CH3)3)4. However, the unexpected preparation of the ligand halfbreed Fe4(NO)4(μ3-S)2(μ3-NC(CH3)3)2 complex allows an evaluation of the effect of bridging-ligand substitution on the structural parameters of cubane-like molecules and presents a unique opportunity to make comparisons between sulfur-bridged and RN-bridged structures within the same molecule. Furthermore, a comparison between the cubane-like Fe4S4 geometry of the Fe4(NO)4(μ3-S)4 molecule and that of the [Fe4(SCH2-C6H5)4(μ3-S)4]2- anion,[2] the first well-defined synthetic analog of the Fe4S4* clusters in high-potential iron protein and in bacterial ferredoxins,[3] has provided addi-

tional important stereochemical evidence relating to their different Fe4S4-core electronic configurations which are dictated by the nature of the terminal ligands.

Fe4(NO)4(μ3-S)4 was prepared by the reaction of [Fe(CO)3NO]2Hg with elemental sulfur in refluxing toluene for 16 hr under nitrogen, while Fe4(NO)4-(μ3-S)2(μ3-NC(CH3)3)2 is similarly formed with {(CH3)3-CN}2S in refluxing benzene for 2 hr. Each of these compounds was isolated and purified by chromatography on silica gel. The diamagnetism of Fe4(NO)4-(μ3-S)4 was established by the nmr method which showed no shift of the ^{1}H resonance of the internal standard tert-butyl alcohol (ca. 2%) in CDCl3. Similarly, the expected diamagnetism of Fe4(NO)4(μ3-S)2-(μ3-NC(CH3)3)2 was substantiated from its ^{1}H nmr spectrum in CCl4 solution showing a sharp singlet at τ 8.52 (vs. TMS internal). Solid-state infrared spectra (KBr pellet) gave one nitrosyl band at 1780 cm^{-1} (s) for Fe4(NO)4(μ3-S)4 and three nitrosyl bands at 1745 (s), 1760 (vs), and 1792 cm^{-1} (w) for Fe4(NO)4(μ3-S)2-(μ3-NC(CH3)3)2.

X-Ray structural determinations carried out for both compounds[4,5] revealed discrete cubane-like molecules sufficiently separated from one another such that the observed molecular parameters (whose important mean values are summarized under the determined chemically equivalent symmetry in Table I for these and two other Fe4S4 clusters) are deemed not to be markedly influenced by crystal packing effects.

The geometry of Fe4(NO)4(μ3-S)4 (Figure 1), which

(2) B. A. Averill, T. Herskovitz, R. H. Holm, and J. A. Ibers, J. Amer. Chem. Soc., 95, 3523 (1973).

(3) C. W. Carter, Jr., J. Kraut, S. T. Freer, R. A. Alden, L. C. Sieker, E. Adman, and L. H. Jensen, Proc. Nat. Acad. Sci. U. S., 69, 3526 (1972).

(4) (a) Fe4(NO)4(μ3-S)4: monoclinic P21/n; a = 12.350 (3), b = 9.627 (7), c = 10.407 (4) Å, β = 103.66 (3)°; V = 1202.3 Å3; ρcalcd = 2.59 g cm^{-3} for Z = 4. Anisotropic least-squares refinement gave R1(F) = 3.2% and R2(F) = 4.2% for 1376 independent diffractometry data (I > 2σ(I)). (b) Fe4(NO)4(μ3-S)2(μ3-NC(CH3)3)2: monoclinic, P21/m; a = 11.140 (2), b = 11.013 (2), c = 7.921 (1) Å; β = 91.82 (1)°; V = 971.4 Å3; ρobsd = 1.85 (5) g cm^{-3} vs. ρcalcd = 1.89 g cm^{-3} for Z = 2. Anisotropic least-squares refinement gave R1(F) = 3.3% and R2(F) = 4.6% for 1194 independent diffractometry data (I > 2σ(I)).

(5) For computation of bond distances and angles, atomic coordinates will appear following these pages in the microfilm edition of this volume of the journal.

has no imposed crystallographic constraints, complies almost exactly with cubic T_d symmetry with the iron atoms forming a completely bonding tetrahedron of 2.634 Å (av). The 12 chemically equivalent Fe–S bond lengths vary from only 2.208 (2) to 2.224 (2) Å with a mean of 2.217 Å. The four Fe–NO bond lengths (of range 1.661 (5)–1.666 (5) Å) are of average length 1.663 Å, while the N–O bond lengths (of range 1.143 (6)–1.171 (6) Å) are of average length 1.152 Å. The essentially linear linkage of each nitrosyl ligand to its iron atom, shown from the 176.9 (5)–178.7 (5)° range for the four Fe–N–O angles, is in accord with the electronic configuration resulting from the localized C_{3v} environment about each iron atom.

The molecular configuration of Fe$_4$(NO)$_4$(μ_3-S)$_2$-(μ_3-NC(CH$_3$)$_3$)$_2$, depicted in Figure 2, has an idealized C_{2v} geometry with one vertical mirror plane crystallographically required. In order to analyze the observed variations in Fe–Fe distances (Table I) of the completely bonding iron tetrahedron, it is convenient to consider the Fe$_4$S$_2$N$_2$ core as comprised of an Fe$_2$S$_2$ fragment fused with an Fe$_2$N$_2$ one *via* two Fe–S, two Fe–N, and four Fe–Fe bonds to give four chemically equivalent Fe$_2$SN fragments. From Table I it is apparent that for the Fe$_2$S$_2$ fragment the distances (especially the Fe–Fe bond length of 2.642 (1) Å) and bond angles compare favorably with the corresponding ones in Fe$_4$(NO)$_4$-(μ_3-S)$_4$. The Fe–Fe bond length of 2.496 (1) Å in the Fe$_2$N$_2$ fragment is expectedly shorter by 0.15 Å, while the intermediate Fe–Fe bond lengths of mean 2.562 (1) Å in the four chemically equivalent Fe$_2$SN fragments are virtually identical with the calculated value of 2.57 Å from an averaging of the Fe–Fe bond lengths for the Fe$_2$S$_2$ and Fe$_2$N$_2$ fragments. Of particular interest is that both symmetry kinds of Fe–S bonds in Fe$_4$(NO)$_4$-(μ_3-S)$_2$(μ_3-NC(CH$_3$)$_3$)$_2$ possess equivalent values of 2.22 Å, analogous to the Fe–S bond lengths in other iron-sulfur clusters containing triply bridging sulfur ligands (*e.g.*, Fe$_3$(CO)$_9$(μ_3-S)$_2$ (2.230 (1) and 2.243 (1) Å)[6a] but significantly shorter than the Fe–S bond lengths in various sulfur-bridged iron dimers (*e.g.*, Fe$_2$(NO)$_4$(μ_2-SC$_2$H$_5$)$_2$ (2.270 (4) Å)[6b] and Fe$_2$(CO)$_6$(μ_2-SR)$_2$ (2.259 (7) Å for R = C$_2$H$_5$[6c] and 2.270 (2) Å for R = C$_6$H$_5$[6d]). An analogous Fe–N bond length trend is found to exist between nitrogen atoms coordinated to three iron atoms *vs.* those attached to two iron atoms. The coordination of each of the three independent nitrosyl ligands is linear with Fe–NO bond lengths of range 1.653 (6)–1.668 (6) Å, N–O bond lengths of range 1.158 (8)–1.173 (7) Å, and Fe–N–O bond angles of range 177.8 (4)–179.4 (7)°.

The qualitative MO metal cluster scheme utilized[1] to describe the bonding in Co$_4$(NO)$_4$(μ_3-NC(CH$_3$)$_3$)$_4$ can be carried over to Fe$_4$(NO)$_4$(μ_3-S)$_4$ to give the electronic configuration (e + t$_1$ + t$_2$)^{16} (a$_1$ + e + t$_2$)^{12} (t$_1$ + t$_2$)^0 with the strongly bonding tetrametal cluster orbitals (a$_1$ + e + t$_2$) completely filled and the highly antibonding tetrametal cluster orbitals (t$_1$ + t$_2$) empty. The dissimilarity of the triply bridging ligands in Fe$_4$-(NO)$_4$(μ_3-S)$_2$(μ_3-NC(CH$_3$)$_3$)$_2$, which lowers the molecular symmetry to C_{2v}, does not allow a convenient applica-
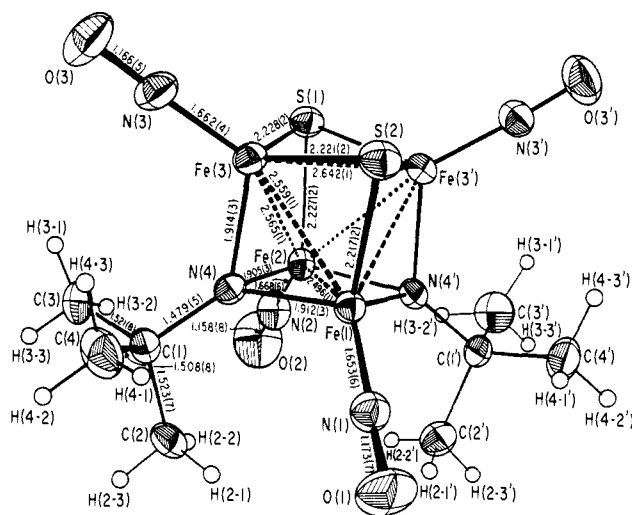

Figure 2. The cubane-like Fe$_4$(NO)$_4${(μ_3-S)$_2$(μ_3-NC(CH$_3$)$_3$)$_2$} molecule of idealized C_{2v}-2*mm* geometry with crystallographic site symmetry C_s-*m* is drawn with 30% probability thermal ellipsoids for the nonhydrogen atoms.

tion of this MO model, but nevertheless it is apparent that the strongly bonding tetrairon orbitals are still completely filled and the corresponding antibonding ones still empty.

The transmutation of Fe$_4$(NO)$_4$(μ_3-S)$_4$ into Fe$_4$(η-C$_5$H$_5$)$_4$(μ_3-S)$_4$[7] by replacement of the four three-electron-donating nitrosyl ligands with four five-electron-donating cyclopentadienyl ligands is shown from Table I to cause a dramatic increase in four of the six Fe–Fe distances from bonding to nonbonding values along with a distortion of the Fe$_4$S$_4$ core from cubic T_d to tetragonal D_{2d} symmetry. These major alterations in the Fe$_4$S$_4$ core, due to the formal addition of eight electrons from the above substitution of four cyclopentadienyl ligands in place of four nitrosyl ones, are readily accommodated in the MO metal cluster model[8] which predicts qualitatively that the addition of eight electrons to the highly antibonding (t$_1$ + t$_2$) tetrairon orbitals of Fe$_4$(η-C$_5$H$_5$)$_4$(μ_3-S)$_4$ gives rise to a first-order Jahn–Teller distortion to tetragonal D_{2d} geometry; the maintenance of two short Fe–Fe distances of 2.65 Å in Fe$_4$(η-C$_5$H$_5$)$_4$(μ_3-S)$_4$ is compatible with the eight antibonding metal cluster electrons being localized between the other four pairs of iron atoms (thereby producing nonbonding distances with valence bond orders of "zero" *vs.* "one" for the two short Fe–Fe bonds). This comparison clearly illustrates the two-electron difference in donating ability between a nitrosyl and a η-C$_5$H$_5$ ligand in a metal cluster system.

Of special interest is a comparison of the geometry of Fe$_4$(NO)$_4$(μ_3-S)$_4$ with that of the [Fe$_4$(SR)$_4$(μ_3-S)$_4$]$^{2-}$ dianion (where R = CH$_2$C$_6$H$_5$) shown by Holm, Ibers, and coworkers[2] from elaborate physical measurements by a number of techniques to be the first well-defined synthetic analog of the class of Fe–S proteins containing Fe$_4$S$_4$ cores. Their suggested qualitative bonding model for this high-spin iron cluster system assumes under T_d symmetry the electronic configuration (a$_1$ + e + t$_2$)^{12}

(6) (a) J. R. Huntsman and L.. F. Dahl, to be submitted for publication; (b) J. T. Thomas, J. H. Robertson, and E. G. Cox, *Acta Crystallogr.*, 11, 599 (1958); (c) L. F. Dahl and C. H. Wei, *Inorg. Chem.*, 2, 328 (1963); (d) W. Henslee and R. E. Davis, *Cryst. Struct. Commun.*, 1, 403 (1972).

(7) (a) R. A. Schunn, C. J. Fritchie, Jr., and C. T. Prewitt, *Inorg. Chem.*, 5, 892 (1966); (b) C. H. Wei, G. R. Wilkes, P. M. Treichel, and L. F. Dahl, *ibid.*, 5, 900 (1966).

(8) B. K. Teo and L. F. Dahl, to be submitted for publication.

$(e + t_1 + t_2)^{10} (t_1 + t_2)^0$ with the ten electrons in the $(e + t_1 + t_2)$ tetrairon orbitals (which are not involved in direct Fe–Fe interactions and hence are essentially nonbonding relative to the direct tetrairon interactions) antiferromagnetically interacting with one another through the triply bridging sulfur atoms.[2,9] It is our prejudice that the observed dimensional differences (Table I) between the Fe_4S_4 cores of $Fe_4(NO)_4(\mu_3\text{-}S)_4$ and the $[Fe_4(SCH_2C_6H_5)_4(\mu_3\text{-}S)_4]^{2-}$ dianion provide definite support for this electronic configuration. The Fe_4S_4 core of the $[Fe_4(SCH_2C_6H_5)_4(\mu_3\text{-}S)_4]^{2-}$ dianion exhibits a definite departure from cubic T_d to tetragonal D_{2d} geometry which is manifested by the occurrence of of the Fe–S bond lengths as two sets of four (2.239 (2) Å) and eight (2.310 (3) Å).[2] The fact that these latter Fe–S distances are 0.09 Å longer than those in Fe_4-$(NO)_4(\mu_3\text{-}S)_4$ is consistent with the premise that the antiferromagnetic interaction in the Fe_4S_4 core of the dianion occurs through antibonding metal–sulfur orbitals. The tetragonal D_{2d} distortion then presumably reflects a metal–ligand induced Jahn–Teller effect (rather than a tetrametal induced one) which in turn produces the observed four equivalent Fe–Fe bonds (2.731 (1) Å) and two slightly longer ones (2.776 (2) Å); these six Fe–Fe distances, which are only 0.10 and 0.15 Å longer than those in $Fe_4(NO)_4(\mu_3\text{-}S)_4$, are thereby indicative of a completely bonding iron tetrahedron in accord with the proposed electronic configuration.

The following qualitative bonding descriptions are outlined for $Fe_4(NO)_4(\mu_3\text{-}S)_4$, the $[Fe_4(SR)_4(\mu_3\text{-}S)_4]^{2-}$ dianion, and $Fe_4(\eta\text{-}C_5H_5)_4(\mu_3\text{-}S)_4$ in order to distinguish clearly their different electronic configurations. In $Fe_4(NO)_4(\mu_3\text{-}S)$ each iron possesses a d^7 Fe(I) configuration by virtue of its coordination with one terminal NO^+ and three triply bridging S^{2-} ligands. The resulting ligand field coupled with the previously described direct metal–metal interactions splits the 20 tetrairon cluster orbitals (constructed from the five 3d AO's of each of the four irons) under assumed T_d geometry such that the 28 valence core electrons available from the four irons produce the electronic configuration $(e + t_1 + t_2)^{16} (a_1 + e + t_2)^{12} (t_1 + t_2)^0$.

In the $[Fe_4(SR)_4(\mu_3\text{-}S)_4]^{2-}$ dianion, a bookkeeping of valence electrons formally leads to the experimentally indistinguishable two d^6 Fe(II) and two d^5 Fe(III). The resulting 22 iron core electrons produce the ground state $(a_1 + e + t_2)^{12} (e + t_1 + t_2)^{10} (t_1 + t_2)^0$ due to the strong stabilization (from the bonding Fe–Fe interactions) of the bonding $(a_1 + e + t_2)$ tetrairon levels *below* and the corresponding antibonding $(t_1 + t_2)$ tetrairon levels *above* the nonbonding $(e + t_1 + t_2)$ tetrairon levels. In contradistinction to the relatively weak ligand effects of the non-π-acidic terminal SR^- ligands, the strong π-acidic effects of the NO^+ ligands have been shown from a (Fenske–Hall)-type molecular orbital calculation[10] of $Fe_4(NO)_4(\mu_3\text{-}S)_4$ to depress the $(e + t_1 + t_2)$ tetrairon levels to lower energies than the $(a_1 + e + t_2)$ tetrairon ones.

In the $Fe_4(\eta\text{-}C_5H_5)_4(\mu_3\text{-}S)_4$ molecule the cyclopentadienyl and sulfide anions procreate four d^5 Fe(III); the interaction of the filled, doubly degenerate localized e_1 (C_5H_5) orbitals, which transform under T_d geometry as $(e + t_1 + t_2)$, with the corresponding higher energy $(e + t_1 + t_2)$ tetrairon orbitals gives rise to *filled* bonding metal–cyclopentadienyl $(e + t_1 + t_2)$ combinations (of predominantly cyclopentadienyl orbital character) and *empty* antibonding metal–cyclopentadienyl $(e + t_1 + t_2)$ combinations (of mainly iron 3d orbital character). Hence, the 20 available iron core electrons are distributed among the 20 3d iron cluster orbitals in the energy order of $(a_1 + e + t_2)^{12} (t_1 + t_2)^8 (e + t_1 + t_2)^0$.

A *high-spin* Fe_4S_4 cluster system thereby corresponds to the bonding tetrametal $(a_1 + e + t_2)$ levels being lower in energy than the *partially occupied* $(e + t_1 + t_2)$ levels, whereas $Fe_4(NO)_4(\mu_3\text{-}S)_4$ and $Fe_4(\eta\text{-}C_5H_5)_4(\mu_3\text{-}S)_4$ may be classified as *low-spin* Fe_4S_4 cluster systems with the $(e + t_1 + t_2)$ tetrametal cluster levels being completely filled in $Fe_4(NO)_4(\mu_3\text{-}S)_4$ and empty in Fe_4-$(\eta\text{-}C_5H_5)_4(\mu_3\text{-}S)_4$.

It is apparent from these considerations that the resulting electronic configurations of $Fe_4(NO)_4(\mu_3\text{-}S)_4$, $[Fe_4(\eta\text{-}C_5H_5)_4(\mu_3\text{-}S)_4]^n$ ($n = 0, +1, +2$), and the $[Fe_4$-$(SR)_4(\mu_3\text{-}S)_4]^{n-}$ anions ($n = 1, 2, 3$) are grossly dissimilar from one another in accord with their widely different chemical and physical properties. These results emphasize that in making stereochemical comparisons of metal cluster systems, one must carefully consider the nature of bonding of the terminal and bridging ligands with respect to their influence upon the energetics of the metal cluster orbitals.

One important manifestation of the specific electronic configuration of the $[Fe_4(SR)_4(\mu_3\text{-}S)_4]^{2-}$ dianion is that either a one-electron oxidation to the monoanion or a one-electron reduction to the trianion should not appreciably alter the Fe–Fe distances of the completely bonding iron tetrahedron in that such electronic changes would involve the $(e + t_1 + t_2)$ tetrairon orbitals which are essentially nonbonding with respect to the direct tetrairon interactions; hence, any observed modification of the tetrairon architecture due to an electron transfer would be mainly an effect of the resulting electronic perturbation directed primarily at the Fe–S framework. Likewise, no pronounced bond-length changes within the completely bonding iron tetrahedron of the electronically analogous $Fe_4S_4^*$ chromophores of the high-potential iron protein and of the bacterial ferredoxins would be expected as a structural consequence of their undergoing one-electron redox reactions. In striking contrast, oxidations of the neutral Fe_4-$(\eta\text{-}C_5H_5)_4(\mu_3\text{-}S)_4$ molecule to the monocation and dication have been shown experimentally from crystallographic studies[11] to deform appreciably the central Fe_4S_4 core in complete harmony with the removal of electrons from the highly antibonding tetrairon cluster orbitals. Similarly, the electronic configuration of the $Fe_4(NO)_4(\mu_3\text{-}S)_4$ molecule allows the prediction[8] that a one-electron reduction to the monoanion should significantly deform its Fe_4S_4 skeleton from a cubic T_d to a tetragonal D_{2d} geometry with *four* longer and *two* shorter Fe–Fe bond lengths.

Cyclic voltammetry on $Fe_4(NO)_4(\mu_3\text{-}S)_4$ and Fe_4-$(NO)_4(\mu_3\text{-}S)_2(\mu_3\text{-}NC(CH_3)_3)_2$ has shown the existence

(9) The same conclusions concerning the electronic configuration of the $[Fe_4(SCH_2C_6H_5)_4(\mu_3\text{-}S)_4]^{2-}$ dianion were reached independently by us.[8]

(10) C. F. Campana, C. T.-W. Chu, and L. F. Dahl, to be submitted for publication.

(11) (a) Trinh-Toan, W. P. Fehlhammer, and L. F. Dahl, Abstracts, 161st National Meeting of the American Chemical Society, Los Angeles, Calif., March 28–April 2, 1971, No. INOR-130; submitted for publication; (b) Trinh-Toan, B. K. Teo, J. A. Ferguson, T. J. Meyer, and L. F. Dahl, submitted for publication.

of both a one-electron oxidation and a one-electron reduction for the former molecule and four one-electron reduction steps for the latter molecule. Attempts to prepare, isolate, and characterize these species are presently in progress.

Supplementary Material Available. A listing of atomic coordinates will appear following these pages in the microfilm edition of this volume of the journal. Photocopies of the supplementary material from this paper only or microfiche (105 × 148 mm, 24× reduction, negatives) containing all of the supplementary material for the papers in this issue may be obtained from the Journals Department, American Chemical Society, 1155 16th St., N.W. Washington, D. C. 20036. Remit check or money order for $3.00 for photocopy or $2.00 for microfiche, referring to code number JACS-74-4019.

Robert S. Gall, Cynthia Ting-Wah Chu, Lawrence F. Dahl*

*Department of Chemistry, University of Wisconsin
Madison, Wisconsin 53706*
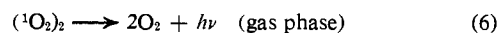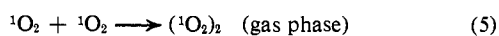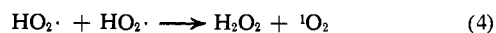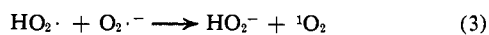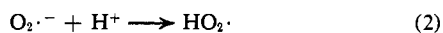
Received February 14, 1974

Singlet Oxygen. The Suppression of Its Production in Dismutation of Superoxide Ion by Superoxide Dismutase

Sir:

We have recently shown that the homogeneous electron transfer between superoxide ion, $O_2 \cdot^-$, and a radical cation, $R \cdot^+$ (*e.g.*, ferricenium cation), produces singlet oxygen.[1] The occurrence of both superoxide ion and singlet oxygen in biological systems has been a topic of recent interest. Fridovich[2] discovered the enzyme superoxide dismutase (SOD, also called erythrocuprein), which catalyzes the dismutation reaction (1)

$$2O_2 \cdot^- + 2H^+ \longrightarrow H_2O_2 + O_2 \qquad (1)$$
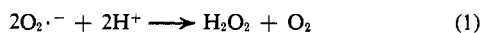
and apparently serves in the defense mechanism of organisms against the potential toxicity of superoxide ion or radicals generated from its decomposition. Stauff and coworkers[3] observed a very weak emission at 630 nm, characteristic of the dimeric $^1\Delta_g$ state of O_2, from the dismutation of superoxide ion in the presence of proton donors. They proposed the following reaction scheme to account for the results.

$$O_2 \cdot^- + H^+ \longrightarrow HO_2 \cdot \qquad (2)$$

$$HO_2 \cdot + O_2 \cdot^- \longrightarrow HO_2^- + {}^1O_2 \qquad (3)$$

$$HO_2 \cdot + HO_2 \cdot \longrightarrow H_2O_2 + {}^1O_2 \qquad (4)$$

$${}^1O_2 + {}^1O_2 \longrightarrow ({}^1O_2)_2 \quad \text{(gas phase)} \qquad (5)$$

$$({}^1O_2)_2 \longrightarrow 2O_2 + h\nu \quad \text{(gas phase)} \qquad (6)$$

In the most recent work of Stauff and coworkers,[4]

(1) E. A. Mayeda and A. J. Bard, *J. Amer. Chem. Soc.*, **95**, 6223 (1973).
(2) I. Fridovich, *Accounts Chem. Res.*, **5**, 321 (1972).
(3) J. Stauff, H. Schmidkeenz, and G. Hartmann, *Nature (London)*, **198**, 281 (1963).

emission during dismutation of superoxide ion was absent, and they suggest the previously observed emission in the blue-green region was attributable to contamination by atmospheric CO_2 and the intermediate involvement of carbonate or bicarbonate radicals.

We report here, by the use of 1,3-diphenylisobenzofuran (DPBF) as a trapping agent, that singlet oxygen is produced by the dismutation of superoxide ion and that this production is greatly decreased in the presence of SOD. The results further show that SOD does not quench singlet oxygen directly but apparently interferes with its production in the dismutation step itself.

Solutions of superoxide ion were produced by reducing oxygen electrolytically with a platinum gauze electrode in a 0.2 M solution of tetra-n-butylammonium perchlorate (TBAP) in dry acetonitrile (35 ml). The reduction was carried out at a potential of -1.6 V *vs.* saturated calomel electrode and the electrolysis of 100 min duration was discontinued after 18 mF were passed. To this solution of superoxide ion, 150 mg (0.55 mmol) of DPBF was added and then the cell was covered with a black cloth to prevent possible photochemical reactions. Ten milliliters of water were added slowly with a syringe. The product, o-dibenzoylbenzene (DBB), was isolated by column and thin-layer chromatography and identified by comparison of ir spectra and R_F values with an authentic sample.

The experiments were repeated utilizing identical conditions as before except that the water (10 ml) contained 0.5 mg of SOD (from bovine red blood cells). Finally, since DPBF can react slowly with ground state oxygen, control experiments were performed to determine the contribution from this pathway. Oxygen was bubbled through a solution of 0.2 M TBAP in acetonitrile for 20 min. Then 150 mg of DPBF was added and the flask was covered with a black cloth. Water (10 ml) was added slowly and the yield of DBB was determined. The results are summarized in Table I. Control experiments described in our paper[1] showed

Table I. Yield of o-Dibenzoylbenzene (DBB) for Superoxide Dismutation in Absence and Presence of SOD

Conditions	Mean yield DBB (mg)	Standard deviation (mg)	% DPBF conversion	No. of trials
$O_2 \cdot^- + DPBF + H_2O$	5.1	1.9	3.1	3
$O_2 \cdot^- + DPBF + H_2O + SOD$	0.5	<0.1	0.3	2
Control experiment				
$O_2 + H_2O + DPBF$	1.5	1.0	0.9	3

that a reaction between $O_2 \cdot^-$ and DPBF to form appreciable amounts of DBB does not occur.

The data in Table I indicate that singlet oxygen is produced from the dismutation of superoxide ion and that SOD has a definite inhibitory effect upon its formation. Emission studies at 630 (the $^1\Delta_g{}^1\Delta_g$ state) and at 478 nm (the $^1\Sigma_g{}^+{}^1\Delta_g$ state), upon water addition to the $O_2 \cdot^-$ solution contained in a cell in an Aminco-Bowman spectrophotofluorometer equipped with a Hamamatsu R456 photomultiplier tube, were unsuccessful.

(4) J. Stauff, U. Sander, and W. Jaeschke in "Chemiluminescence and Bioluminescence," M. J. Cormier, D. M. Hercules, and J. Lee, Ed., Plenum Press, New York, N. Y., 1973, p 131.